Properties of Electron Beam Hardened Layers made by Different Beam Deflection

Jiří Matlák, Ivo Dlouhý
Institute of Materials Science and Engineering, NETME centre, Brno University of Technology, Czech Republic,
e-mail: xcmatlakj@fme.vutbr.cz, dlouhy@fme.vutbr.cz

The usage of the high-energy electron beam source enables repeated surface quenching of chosen areas of an engineering part surface. Different techniques of electron beam deflection allow creating of hardened layers of different shapes and thicknesses. Experiments were carried out with 42CrMo4 (1.7225) steel. The deflection modes tested were one-point, 6-point, 11-point, line, field and meander. The influence of process speed and defocusing of the electron beam was also taken into account. The electron beam surface quenching resulted in a very fine martensitic microstructure with a hardness of over 700 HV0.5. The thickness of the hardened layers depends on the deflection mode and is affected directly (except field deflection) by process speed. The maximum hardened depth (NCHD) was 1.49 mm. Electron beam defocusing affects the width of the hardened track and can cause extension of the trace up to 40%. The hardness values continuously decrease from the surface to the material core.

Keywords: Electron beam, surface hardening, 42CrMo4 steel, beam deflection

1 Introduction

Electron beam (EB), together with laser beam, belongs to the advanced technologies that can be used for local surface heat treatment. Both methods have some similar characteristics; however there are clear differences predetermining which of them will be chosen for a particular spplication. The fast beam deflection appears to be one of the typical features of EB processing that allows a different distribution of the supplied energy provided adequate programming of the hardening equipment is applied. An EB can be deflected both in a direction perpendicular to the component movement direction and also in a parallel direction. [1-6]

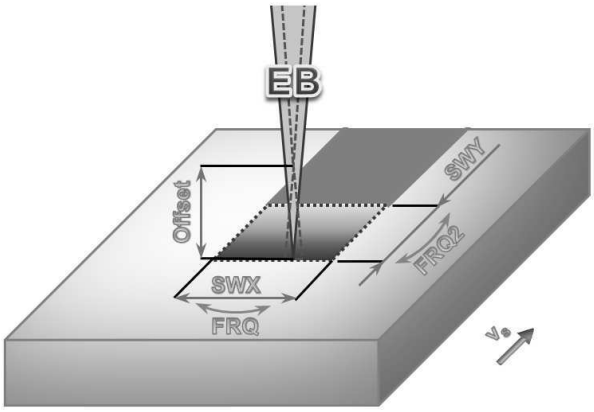

Fig. 1 *The EB surface quenching parameters scheme.*

The properties of the hardened layer can be directly controlled by process parameters. The total supplied power rate is controlled by a combination of the accelerating voltage „UEB“ and the electron current „IEB”. This energy is distributed to the component surface depending on the selected mode of EB deflection. The scanned area is determined by the dimensions „SWX“ and „SWY“ and is set together with the scanning frequency in the individual directions „FRQ“, „FRQ2“ (**Fig. 1**). Usually some beam defocusing „Offset“ is set up, which can be implemented by shifting of the focal plane above the quenched surface (a positive value) or below the surface (a negative value). The last very important parameter is the quenched component movement rate “v_s” under the hardening beam „EB“. [7-14]

2 Experimental material and methods

Experiments were carried out on the high grade 42CrMo4 (1.7225) steel with the following chemical composition of (in wt%): C 0.41, Mn 0.69, Si 0.25, Cr 1.04, Mo 0.20), which is a suitable material for surface hardening. It finds application where elevated strength in combination with a defined and high level of toughness are the most important requirements. The material to be tested was in a state after tempering at 600° C for 3 hours with a final fine sorbitic structure and an average hardness of 300 HV0.5.

The surface quenching was performed using PROBEAM K26 equipment adopting the electron beam technology with a maximum beam power of 15 kW and an accelerating voltage from 80 to 150 kV. The widths of the EB hardened traces were set to be SWX = 10 mm except for one-point deflection. The constant accelerating voltage U_{EB} = 80 kV was used for the experiments and the electron beam current I_{EB} was subsequently optimized for each machine configuration. The EB modes tested were: one-point (stable beam without deflection), 6-point, 11-point, a line (consisting of 1.000 points distributed perpendicular to the “ ”), a field and a meander. Additional processing parameters such as the defocusing degree and the movement rate in each mode and their effect on the quality of the hardened layer were investigated. The common “Offset” values for each mode were 50, 100, 200 and 300 mA and the current sample-to-beam velocities “v_s” were 5, 10, 15, 20 and 25 $mm \cdot s^{-1}$.

The field deflection mode was programmed to allow the local energy density to increase within a given area. This is used for intense heating on the surface of a treated material during the hardening. The rest of the area, with a lower beam intensity, contributes to the heating of the material deeper into the sample core. The length of the SWY field was determined for each movement rate “v_s” based

on the change in temperature across the affected area on the sample measured with a pyrometer.

The meander deflection technique differs from the other ones. The meandering pattern is a combination of the controlled component movement and of the electron beam deflection. The resulting EB trajectory on the specimen surface is shown in **Fig. 2**.

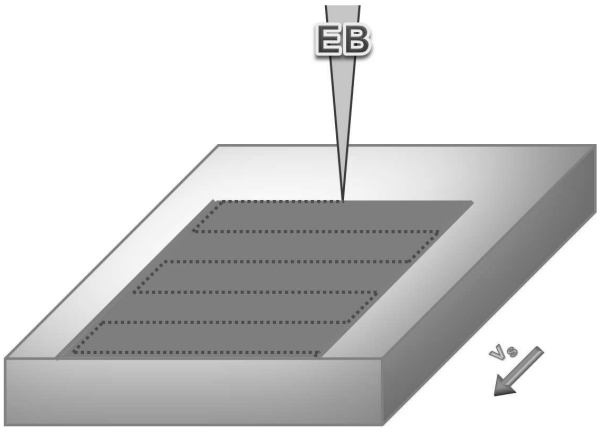

Fig. 2 *The EB trajectory (red dotted line)on specimen surface at the meander deflection.*

The metallographic specimens prepared by standard procedures were analysed by light and the scanning electron microscopy. The LECO LM 247 AT microhardness tester was used to analyse the hardness HV0.5 profile from the surface to the sample core in the hardening trace axis (indented in 3 rows to compliance the obligatory spacing between indentations). For the microstructural characterization, the scanning electron microscope (SEM) ULTRA PLUS, Carl Zeiss GmbH, Germany, equipped with dispersive X-ray spectrometer (EDS) X-MAX, Oxford Instruments, United Kingdom, was used. For the surface analysis, the detector of secondary electrons (SE), type Everhar-Thornley and the four- quadrant silicon detector of back scattered electrons (BSE) were used.

3 Results

Traces having width of 10 mm were processed by a surface quenching on the 42CrMo4 steel. Basic experiments were optimized from the point of view of the used electron beam current I_{EB}. The optimal energy density conditions were specified by the trial and error method based on the observation of the occurrence of molten areas on the specimen surface. The molten areas were brighter than the hadened ones. A slightly molten surface could not be identified by observing the microstructure because it was also formed by a fine martensitic structure similar to hardened layer. The maximum hardness of the hardened and the partially molten material was the same and therefore it could not be used to determine the optimal EB current for hardening.

The length of the field deflection was determined by a pyrometric measurement of the temperature profile within the irradiated area. When too long "SWY" caused a significant drop in temperature, while if too short, it did not exploit all the potential of the EB technology. "SWY" parameters optimized for an individual tested movement rate are given in **Table 1**.

Tab. 1 *Optimal length SWY of the field resulted from temperature profile.*

Movement rate	$mm \cdot s^{-1}$	5	10	15	20	25
Field length	mm	5	8	12	18	25

From the macroscopic point of view, a constant width of traces was observed in the beam movement direction. A continuous hardening depth decrease to the trace edge was observed in the direction perpendicular to the beam movement (**Fig. 4**). The microstructure in the surface hardened area of all the traces consisted of fine martensite (**Fig. 3**). The finest martensite was obtained at the one-point deflection and coarsest martensite at the field mode. The meander deflected martensite looks fine and very similar to the one-point deflection. No significant microstructure difference was observed when applying the 6-point, the 11-point and the line deflection. A continuous change of the fine martensitic structure to the basic material formed by a tempered martensitic structure with carbides was observed in the transition area (**Fig. 5**).

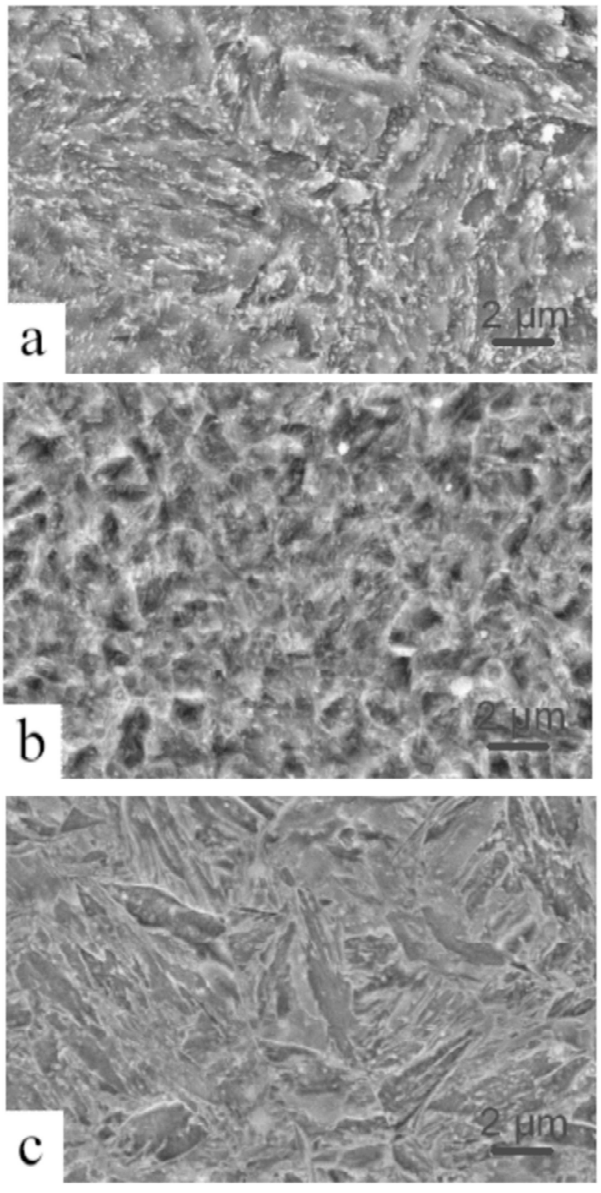

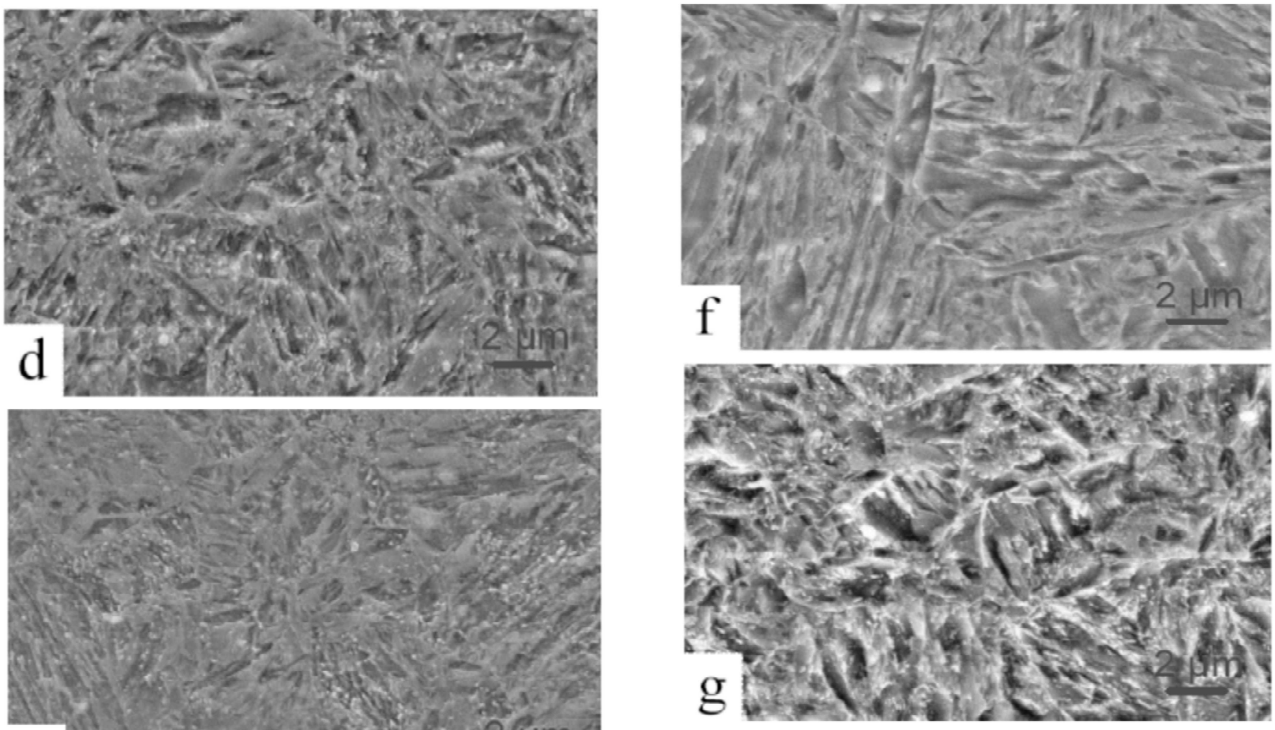

Fig. 3 *The microstructure (SE) of (a) basic material, and hardened layers, (b) one-point, (c) 6-point, (d) 11-point, (e) line, (f) field and (g) meander deflection regimes respectivelly*

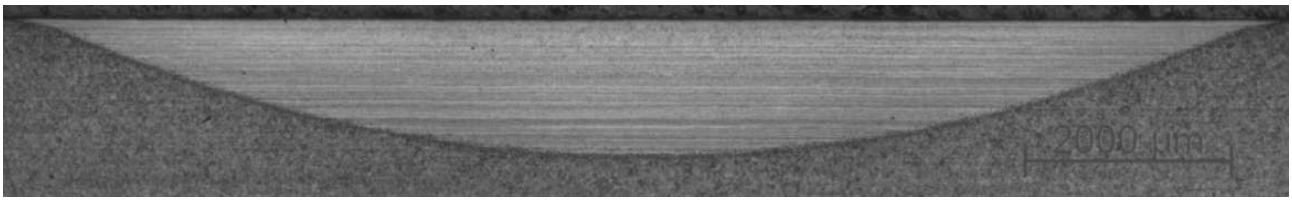

Fig. 4 *The macrostructure of the surface hardened area in a perpendicular direction - field deflection*

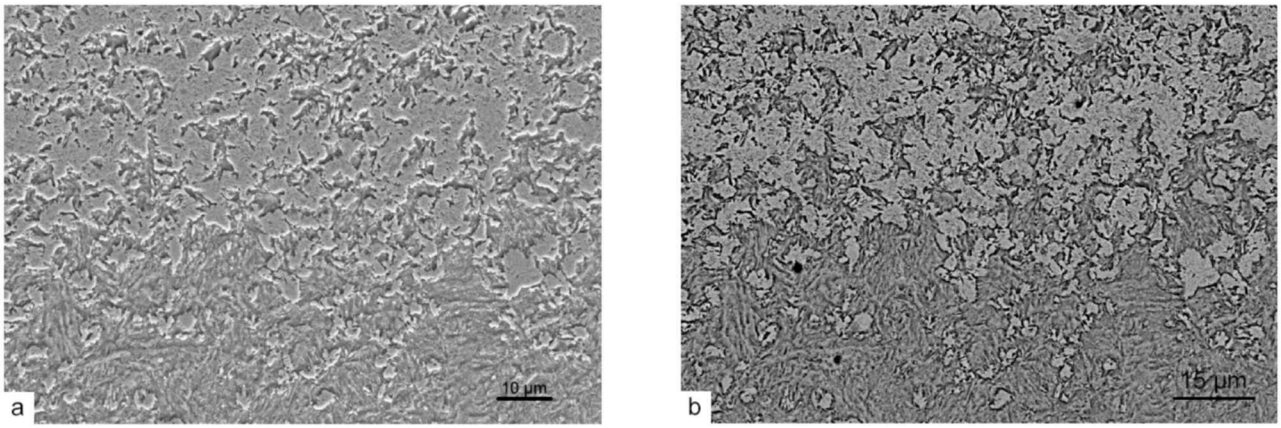

Fig. 5 *The microstructure of the transition area of field deflection sample, (a) SEM – SE mode, (b) SEM – BSE mode*

Fig. 6 *Comparison of the profiles of hardened layers*

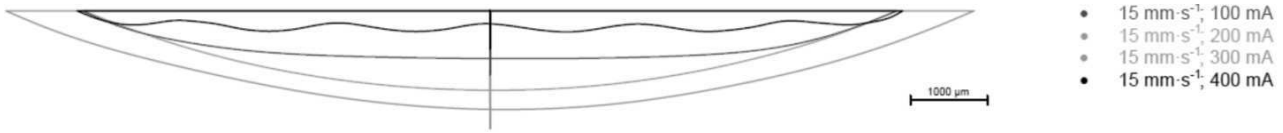

Fig. 7 *The influence of "Offset" on the profiles of the hardened layers –6-point deflection*

A comparison of the profiles of hardened layers made by different deflection modes shows that the lower number of deflected points forms a wider track - Fig. 6 (except the one-point mode). The track made by the field deflection is the deepest one; the shallowest ones are made by the one-point and the meander deflections. The one-point and the field deflections have a significant curvature in comparison to the other deflection modes, which are rather parallel to the surface. Different movement rates have a negligible influence on the trace profile. The "Offset" has a significant effect on the shape of the track. With increasing "Offset" value the trace is becoming wider while, on the contrary, very low "Offset" values lead to easier melting as well as to a significant deformation of the trace profile - Fig. 7

The movement rate "v_s" has only a little effect on the depth of the hardened layer, in particular when applying the one-point, the meander and the field deflection (Fig. 8). For the field deflection, it is the result of optimizing the field length SWY. The depth depends significantly on the movement rate for the 6-point, 11-point and the line deflection and the dependence is nearly identical. The depth gradually increases with decreasing specimen to the electron beam speed and the greatest change can be seen between 5 and 10 mm·s^{-1}.

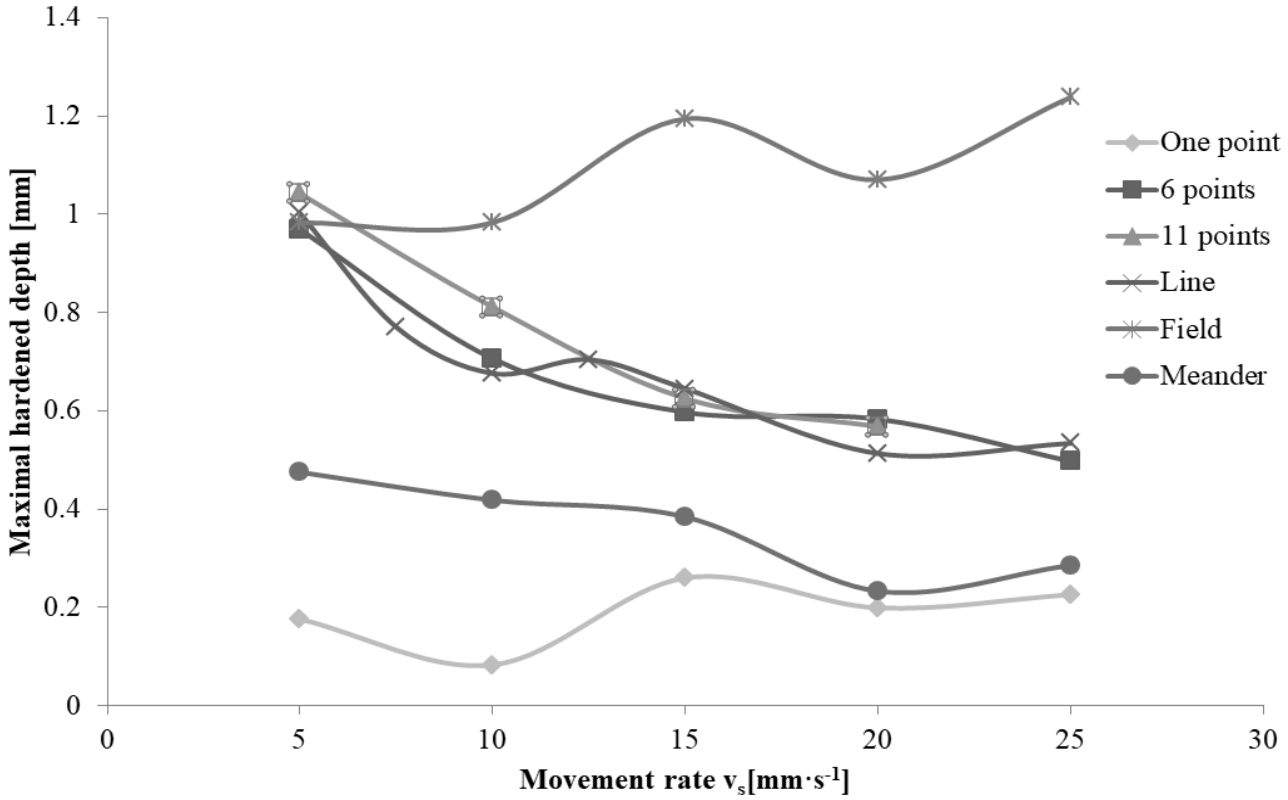

Fig. 8 *The influence of movement rate "v_s" on maximal hardened depth*

An increasing "Offset" leads to an increase in the hardened layer depth (Fig. 9). It is interesting that at higher "Offset" values there is no significant difference between different deflection modes. The one-point and the field deflection differ from the other ones by a poorer response to the "Offset" change.

Maximal hardness values (up to 740 HV0.5) were reached with the one-point deflection because the heating and especially the cooling processes were very fast. Similar values were reached with the meander deflection. The experiments with the other deflection modes give hardness values between 600 and 700 HV0.5. The measured values decreased from the surface to the sample core. A continuous decrease in microhardness was observed on the interface between the quenched area and the basic material. No decrease in microhardness of the basic material was observed in the vicinity of the hardened traces (Fig. 10). Hardness profiles were the same in the middle of the track as closer to the edges (except the different hardening depths).

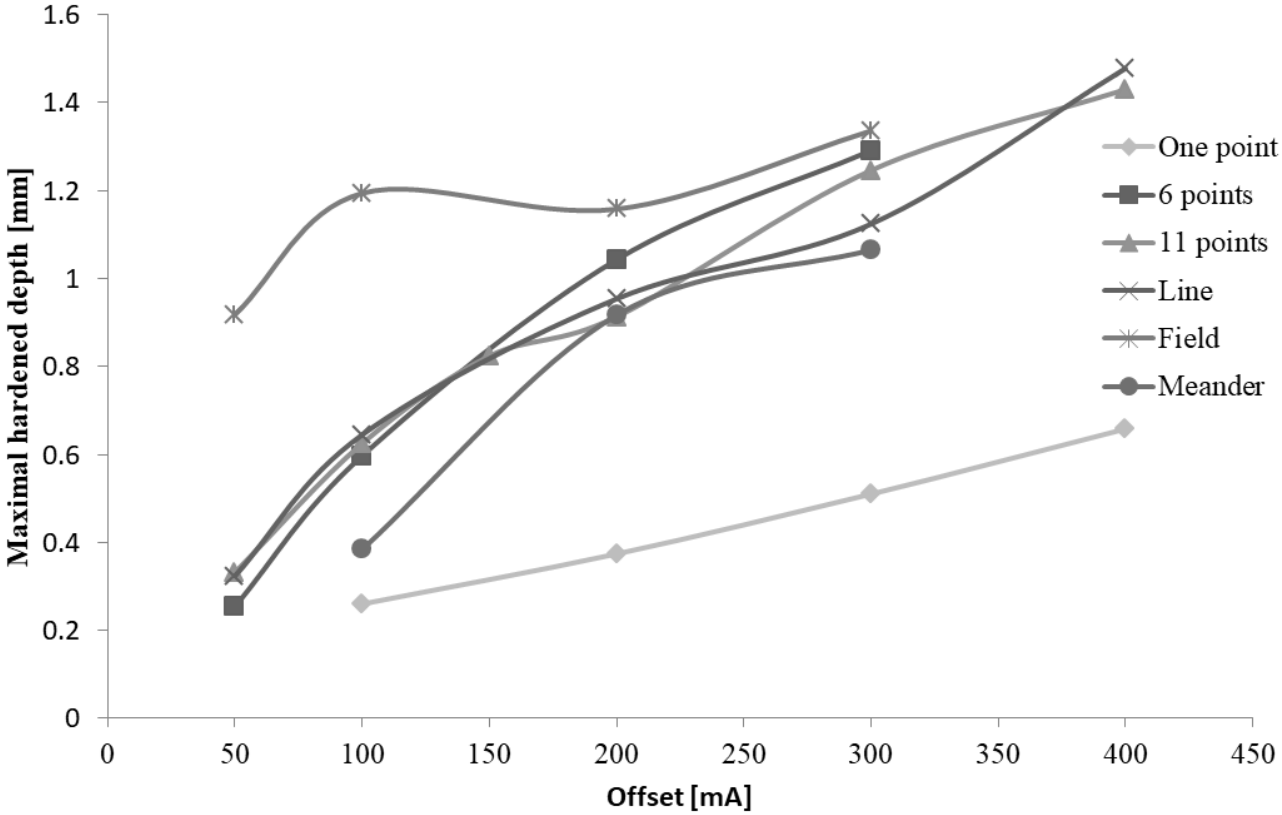

Fig. 9 *The dependence of maximal hardened depth on the defocusing "Offset"*

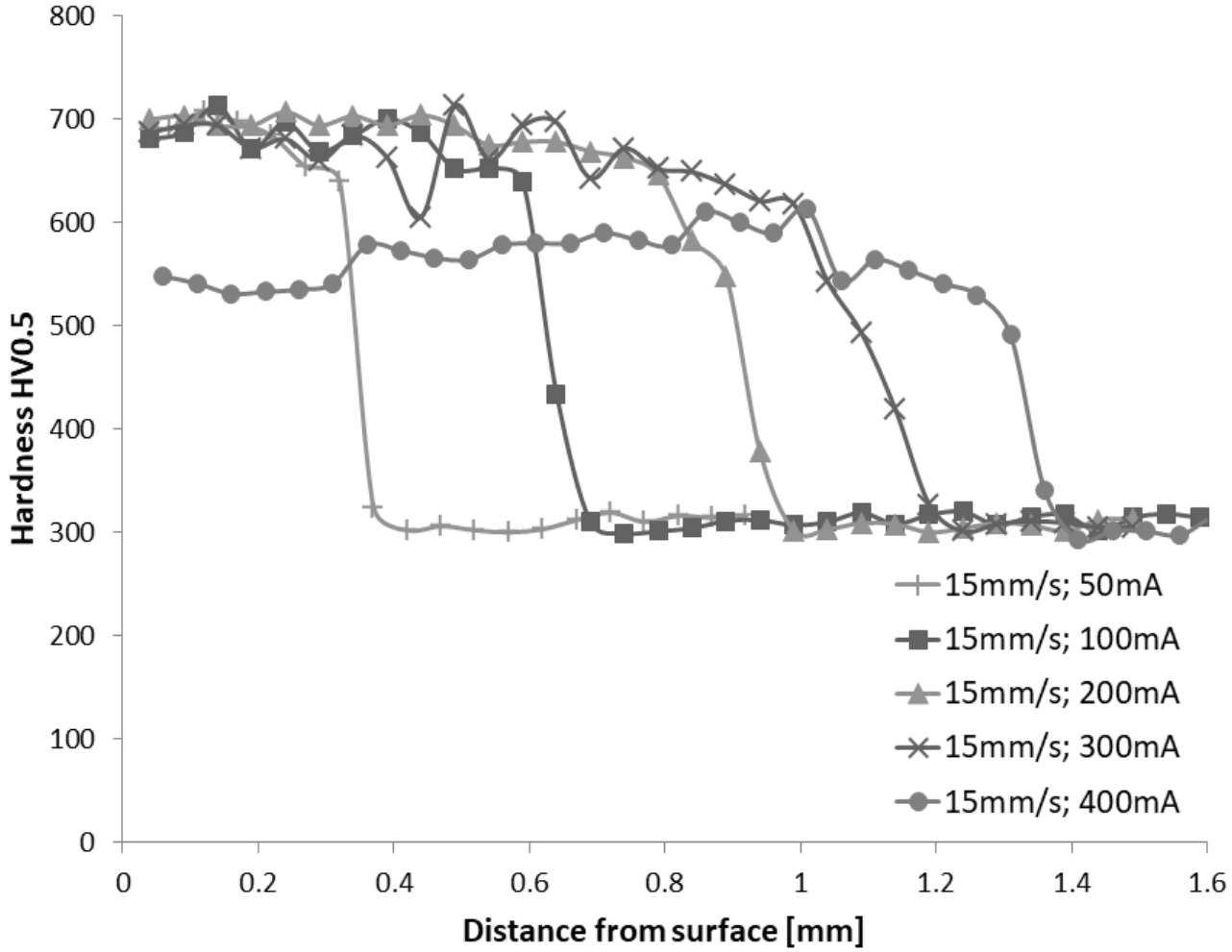

Fig. 10 *The influence of the defocusing "Offset" on the hardness profiles of layers*

It was not confirmed that the movement rate "v_s" affected the final surface hardness. Very high EB defocusing causes a total reduction in the hardness in the entire layer. The "Offset" value 400 mA resulted in an average hardness of 570 HV0.5 of the hardened track and it represents a 20% decrease in comparison with a sharper beam (Fig. 10).

4 Conclusion

The work was focused on a systematic evaluation of the deflection mode (one-point, 6-point, 11-point, line, field, meander) on the surfaces hardened by electron beam. The results showed that the deflection mode can affect a number of track parameters. The martensitic structure is the finest when the one-point and the meander deflection modes are applied. The coarsest structure is generated when applying the field deflection mode. The deflection mode affects the maximum hardness to only a little extent. The highest hardness 740 HV0.5 was observed for the one-point deflection mode. For the other regime modes, the maximum values are near 700 HV0.5.

The geometric profiles in the cross-sections of tracks are different for each of the applied deflection modes. The 6-point, 11-point, the line and the meander deflection mode are parallel to the surface and the one-point mode together with the field mode are significantly curved. The widths of the tracks were similar except for the one-point mode. The depths of hardened layers were in the range 0.1-1.5 mm. The lowest depth of tracks was produced by the one-point deflection mode and the deepest one by the field mode.

The sample-to-electron beam movement rate affects only the depth of the hardened layer. The depth slightly increases with the speed decreasing. The defocusing affects the depth more significantly. Moreover, an increasing "Offset" leads to wider tracks. If the "Offset" is too low, it can severely distort the profile of the hardened layer. Very high values, in turn, lead to an overall reduction in the hardness of the layer and eliminate the profile differences between the different types of deflection.

Acknowledgments

The works have been supported by the project NETME centre plus (Lo1202), project of Ministry of Education, Youth and Sports under the "national sustainability programme".

References

[1] ZENKER, R. (2009). Modern thermal electron beam processes: Research and industrial application. In: *La Metallurgia Italiana*., aprile, S. 8.

[2] MEŠKO, J., ZRAK, A., MULCZYK, K., TOFIL, S. (2014). Microstructure analysis of welded joints after laser welding. In: *Manufacturing Technology*, 2014(3), pp. 355-359. ISSN 1213-2489

[3] DIMITROV, D., APRAKOVA, M., VALKANOV, S., PETROV, P. (1998). Electron beam hardening of iron nitrided layers. In: *Vacuum*, 49 (3), pp. 239-246.

[4] ZENKER, R., SPIES, H.-J., BUCHWALDER, A., SACHER, G. (2006). Combination of thermal surface treatment by high energy beams with thermochemical treatment and hard protective coating – state of the art. In: *Proceedings – 15th IFHTSE – International Federation for Heat Treatment and Surface Endineering Congress 2006*, pp. 214-219.

[5] IVANOV, Y.F., BESSONOV, D.A., VOROB'EV, S.V., GROMOV, V.E., IVANOV, K.V., KOLUBAEVA, Y.A., TSELLERMAER, V.Y. (2013). On the fatigue strength of grade 20Cr13 hardened steel modified by an electron beam. In: *Journal of Surface Investigation*, 7 (1), pp. 90-93.

[6] RADEK, N., MEŠKO, J., ZRAK, A. (2014). Technology of Laser Forming. In: *Manufacturing Technology*. 2014(3), pp. 428-431. ISSN 1213-2489

[7] DUAN, S., QIN, C., LI, B. (2015). Microstructure and properties of semi-HSS treated byl laser quenching. In: *Jinshu Rechuli/Heat Treatment of Metals*, 40 (9), pp. 76-78.

[8] ZENKER, R., BUCHWALDER, A. (2010). *Elektronstrahlrandschichtbehandlung: Inovarive Technologien für höchste Ansprüche*. 2nd edition. Germany: Pro-Beam AG&CO. KGAA.

[9] BREZNIČAN, M., FABIAN, P., MEŠKO, J., DRBÚL, M. (2013). The simulation of influence of quenching temperature on properties of bearing rings. In: *Manufacturing Technology*. 2013(1), pp. 20-25. ISSN 1213-2489.

[10] FRIEDEL, K.P., FELBA, J., POBOL, I., WYMYSLOWSKI, A. (1996). A systematic method for optimizing the electron beam hardening process. In: *Vacuum*, 47 (11), pp. 1317-1324.

[11] VUTOVA, K., DONCHEV, V., VASSILEVA, V., MLADENOV, G. (2014). Thermal processes in electron-beam treatment of metals. In: *Metal Science and Heat*, 55 (11-12), pp. 628-635.

[12] SONG, R.G., ZHANG, K., CHEN, G.N. (2003). Electron beam surface treatment. Part I: Surface hardening of AISI D3 tool steel. In: *User Modeling and User-adapted Interaction*, 69 (4), pp. 513-516.

[13] MATLÁK, J., DOLEŽAL, P., ZAPLETAL, J., VANČURA, F., DLOUHÝ, I. (2016). Electron beam surface quenching of X37CrMoV51 tool steel swages. In: *Manufacturing Technology*. 2016(4), pp. 744-749. ISSN 1213-2489.

[14] BUCHWALDER, A, KLOSE, N., JUNG, A. et al (2016). Improved surface properties of nodular cast iron using electron beam remelting and alloying with nickel based additives. In: Electrotechnica and Electronica E+E. VARNA.

10.21062/ujep/91.2018/a/1213-2489/MT/18/2/279